CHEMISTRY
A EUROPEAN JOURNAL

DOI: 10.1002/chem.201000091

Optically Degradable Dendrons for Temporary Adhesion of Proteins to DNA

Mauri A. Kostiainen,*[a, b] Juha Kotimaa,[c] Marja-Leena Laukkanen,[c] and Giovanni M. Pavan[d]

Abstract: Experimental studies and molecular dynamics modeling demonstrate that multivalent dendrons can be used to temporarily glue proteins and DNA together with high affinity. We describe *N*-maleimide-cored polyamine dendrons that can be conjugated with free cysteine residues on protein surfaces through 1,4-conjugate addition to give one-to-one protein–polymer conjugates. We used a genetically engineered cysteine mutant of class II hydrophobin (HFBI) and a single-chain Fragment variable (scFv) antibody as model proteins for the conjugation reactions. The binding affinity of the protein–dendron conjugates towards DNA was experimentally assessed by using the ethidium bromide displacement assay. The binding was found to depend on the generation of the dendron, with the second generation having a stronger affinity than the first generation. Thermodynamic parameters of the binding were obtained from molecular dynamics modeling, which showed that the high binding affinity for each system is almost completely driven by a strong favorable binding enthalpy that is opposed by unfavorable binding entropy. A short exposure to UV ($\lambda \approx 350$ nm) can cleave the photolabile *o*-nitrobenzyl-linked binding ligands from the surface of the dendron, which results in loss of the multivalent binding interactions and triggers the release of the DNA and protein. The timescale of the release is very rapid and the binding partners can be efficiently released after 3 min of UV exposure.

Keywords: dendrimers · DNA · multivalency · protein modifications · self-assembly

Introduction

The fabrication of highly monodisperse macromolecules with structural anisotropy is an important requirement for achieving materials with predictable complex structures and functions.[1] Recent years have witnessed rapid developments in the synthesis of anisotropic particles, and consequently a rich toolbox of materials with tunable properties is now available.[2] Further variation of these building blocks equipped with "adhesive patches" has considerably expanded the structural variety of possible self-assemblies.[3–6] Much of the recent interest has focused on the assembly of synthetic materials and, therefore, biohybrid materials have received less attention.

Biological systems can offer a vast repository of building blocks already developed by nature that can be functionalized further by attaching synthetic molecules to their surfaces.[7–13] Herein, we report a protein particle functionalized with a DNA adhesive unit that consists of a photoresponsive Newkome-type polyamine dendron with multiple spermine surface groups (Figure 1). Dendritic systems are of particu-

[a] Dr. M. A. Kostiainen
Department of Engineering Physics
Helsinki University of Technology
P.O. Box 2200, 02015 HUT, Espoo (Finland)

[b] Dr. M. A. Kostiainen
Current address: Institute for Molecules and Materials,
Radboud University Nijmegen
Toernooiveld 1, 6525 AJ Nijmegen (The Netherlands)
Fax: (+31) 24-36-53393
E-mail: m.kostiainen@science.ru.nl

[c] J. Kotimaa, Dr. M.-L. Laukkanen
VTT Biotechnology
Tietotie 2, P.O. BOX 1500, 02044 VTT (Finland)

[d] G. M. Pavan
Mathematical and Physical Sciences Research Unit
University for Applied Sciences of Southern Switzerland
Centro Galleria 2, Manno 6928 (Switzerland)

Supporting information for this article is available on the WWW under http://dx.doi.org/10.1002/chem.201000091.

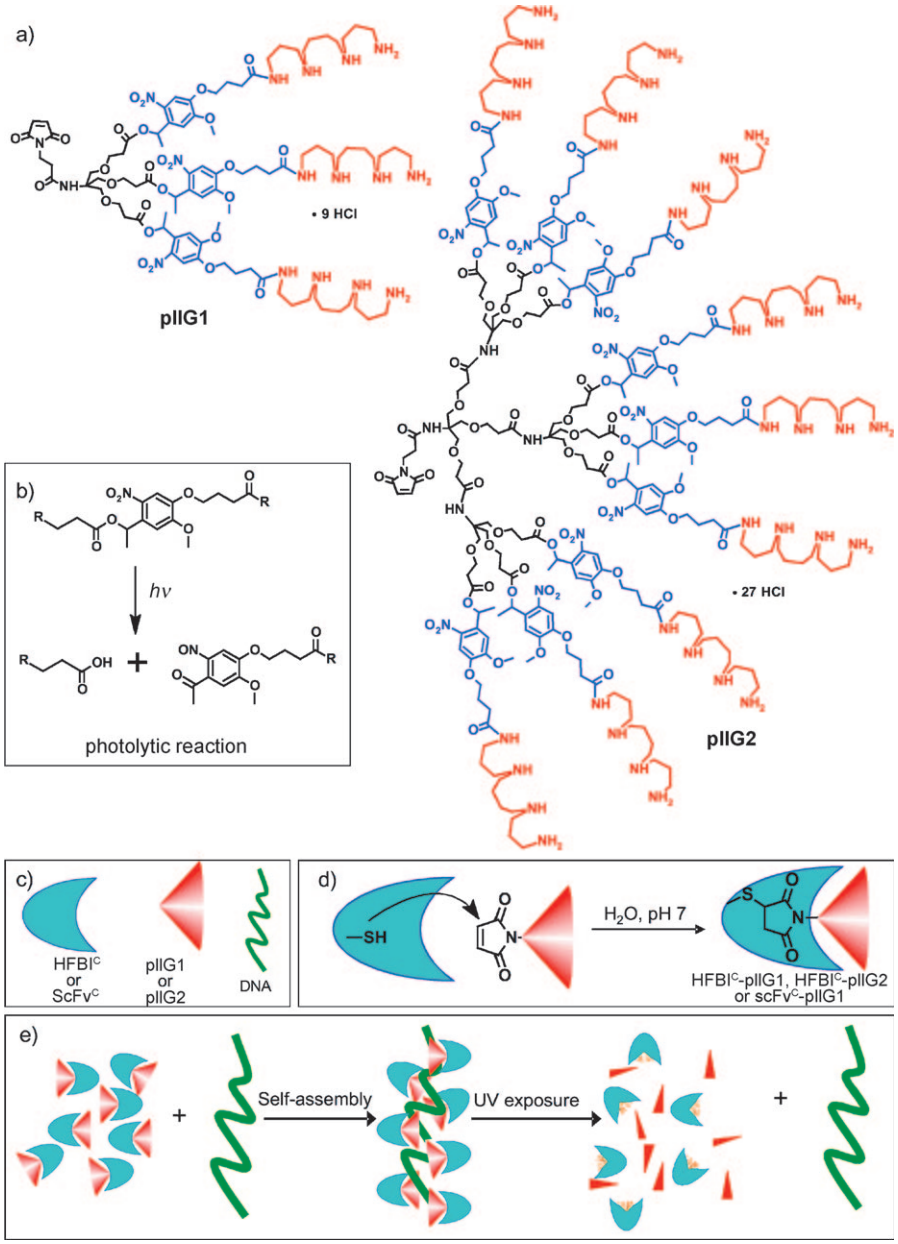

Figure 1. Strategy for the temporary adhesion of proteins to DNA. a) Optically degradable dendrons used for protein conjugation and subsequent DNA binding. b) Schematic representation of the photolytic reaction. c) Symbols key. d) Preparation of protein–dendron conjugates. e) Schematic illustration of the assembly and disassembly process. Photosensitive dendrons bind DNA through electrostatic interactions and "glue" the proteins to the surface of DNA. UV exposure induces the controlled decomposition of dendrons, which results in loss of the multivalent interactions and release of the DNA.

lar interest as multivalent ligand displays because the inherent branching of the scaffold means that the dendritic surface groups naturally form a well-defined multivalent array.[14] Such an array can interact with its binding partner with high affinity.[15–18] Using light as an external stimulus to control the binding interactions of the dendron provides special advantages, such as being highly orthogonal and quick and easy to apply; most importantly, it allows spatiotemporally precise control over the release event.[19–22] DNA-binding and -releasing dendrons are particularly interesting in gene-delivery applications due to their ability to facilitate gene transfection.

Herein, class II hydrophobin (HFBI) from *Trichoderma reesei* was chosen as the protein part.[23–26] HFBI has a very unusual amphiphilic structure in which approximately half of its hydrophobic amino acid sidechains form a hydrophobic patch that is exposed on the protein surface. HFBI can, therefore, be regarded as a mesoscale surfactant protein that can form various structures through spontaneous self-assembly.[27] Furthermore, mesoscale surfactants exhibit very interesting properties in hydrophobic assembly in general.[28] To demonstrate the flexibility of our approach, we also studied an anti-Human Epidermal growth factor Receptor 2 (HER2) single-chain Fragment variable (scFv) antibody for the conjugation reactions. These types of antibody fragments are interesting targeting ligands due to the fact that many cancer types overexpress HER2 on their surfaces and because the antibody binding to HER2 can cause endocytosis of the receptor, thus actively delivering an antibody-conjugated payload inside the cell.

We have previously reported a series of different Newkome-type dendrons with spermine surface groups capable of binding DNA with high affinity.[29,30] The dendrons were further modified to allow their site-specific conjugation on protein surfaces and were shown to act as high-affinity DNA adhesion patches.[31,32] HFBI functionalized with a second-generation spermine dendron was biocompatible and could promote gene transfection in vitro. Finally, we have developed multivalent dendrons that can be degraded with light,[33] pH changes,[34] or reduction[35] to trigger DNA release in a controlled manner. We present a feasible method to prepare anisotropic protein–dendron conjugates in which the dendron can be degraded with optical stimuli. Importantly, we

show that the DNA binding and adhesion of proteins on DNA is fully reversible.

Results and Discussion

Optically degradable dendrons with an *N*-maleimido group at the focal point (**pllG1** and **pllG2**; Figure 1a) were synthesized and characterized by standard methods (see the Supporting Information). The dendrons consist of a Newkome-type branching scaffold that is functionalized with multiple spermine ligands. Each of the spermine ligands is attached to the scaffold by an *o*-nitrobenzyl linker that can be cleaved by UV light to destroy the multivalent binding surface. A *N*-maleimido group at the focal point of dendron is ideal for protein functionalization because it is known to react selectively with free cysteine sulfhydryl groups through 1,4-conjugate addition under mild aqueous conditions. However, native HFBI does not offer free cysteine residues for site-specific conjugation. Therefore, site-directed mutagenesis was used to construct a protein variant of HFBI with a free sulfhydryl group (HFBI^{C}), which can react with the dendron. The HFBI^{C} protein variant was produced in its homologous production host *T. reesei* and purified from the fermentation biomass to give a partially oxidized covalent protein dimer that was subsequently reduced to protein monomers with dithiothreitol. Protein–dendron conjugates were finally assembled by Michael addition reactions between the free cysteine of the protein and the *N*-maleimido group of the dendron (Figure 1d). To demonstrate the generality of our approach, another cysteine-modified protein, scFv^{C}, was prepared by using a similar approach (see the Experimental Section).

HFBI^{C} conjugates were purified by using semi-preparative reversed-phase high-performance liquid chromatography (RP-HPLC) by monitoring $\lambda = 230$ and 380 nm. Absorption at $\lambda = 380$ nm originates from the *o*-nitrobenzyl functionality and is specific for the dendrons. RP-HPLC chromatograms for both HFBI^{C}–**pllG1** (see the Supporting Information) and HFBI^{C}–**pllG2** (Figure 2a) reaction mixtures show the highest peak with a retention volume (V_{ret}) of around 115 mL. This peak clearly shows absorption at both of the monitored wavelengths, indicating the presence of the conjugate, which was further supported by matrix-assisted laser desorption/ionization time-of-flight (MALDI-TOF) mass spectrometry (see the Supporting Information). Peaks with $V_{ret} \approx 115$ mL were fractionated, pooled, and lyophilized to give the products as slightly yellow solids. The high purity of the final products was confirmed by analytical HPLC, which shows a single peak for both compounds (Figure 2b).

The DNA binding and release properties of the conjugates were initially studied with an ethidium bromide (EthBr) displacement assay at physiologically relevant conditions (pH 7.2, 150 mM NaCl). For comparison the binding was also studied at 9.4 mM NaCl. This assay utilizes the competition between the DNA binding ligands and EthBr towards binding of DNA. EthBr exhibits intense fluorescence

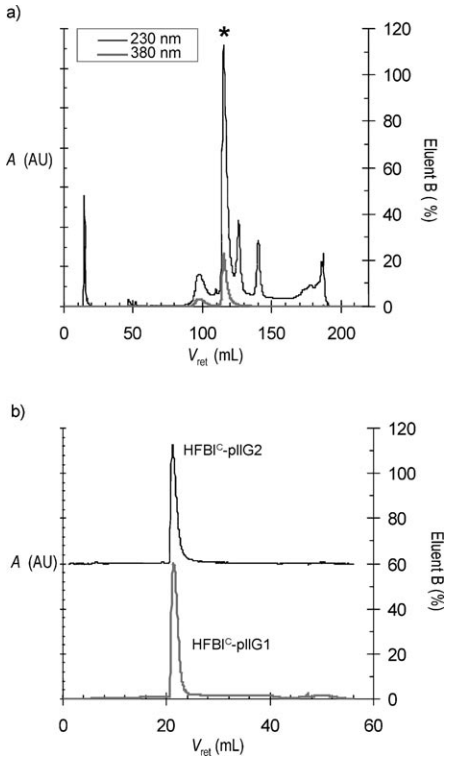

Figure 2. Analytical data for protein–dendron conjugates: a) Semipreparative HPLC chromatogram of the HFBI^{c}–pllG2 reaction mixture. The peak corresponding to HFBI^{C}–**pllG2** is marked with an asterisk. b) Analytical HPLC chromatogram of purified HFBI^{C}–**pllG1** and HFBI^{C}–**pllG2**.

when bound to DNA; however, its fluorescence is quenched when it is displaced from the DNA by a DNA-binding ligand. Binding values are best described by CE_{50} values (see the Experimental Section), which indicate the nominal dendron charge excess that causes a 50% decrease in fluorescence intensity.

Compounds HFBI^{C}–**pllG1** and HFBI^{C}–**pllG2** both show good DNA-binding affinity at both salt concentrations, and are able to displace EthBr from DNA due to strong electrostatic interactions between the dendron and the polyanionic DNA (Figure 3 and Table 1). In the presence of 9.4 mM NaCl, both HFBI^{C}–**pllG1** and HFBI^{C}–**pllG2** are able to bind DNA in similar manner with extremely high affinity, and the CE_{50} value for both compounds is 0.6. The binding affinity of scFv^{C}–**pllG1** ($CE_{50} = 1.3$, see the Supporting Information) is lower than that of the hydrophobin conjugates. A lower affinity might be expected because the size of the scFv^{C} ($\approx$29 kDa) is much larger than that of the HFBI^{C} ($\approx$9 kDa). The binding affinity of an individual spermine ligand is considerably weaker ($CE_{50} = 6$), and unmodified HFBI fails to interact with DNA ($CE_{50} > 200$). Therefore, no quenching of the fluorescence is observed. In the presence of 150 mM NaCl, spermine and HFBI^{C} are unable to bind DNA due to the lack of sufficient electrostatic interactions and consequently fluorescence quenching is not observed. In contrast, the multivalent dendron conjugates are less adversely affected by the increase in NaCl concentration. The

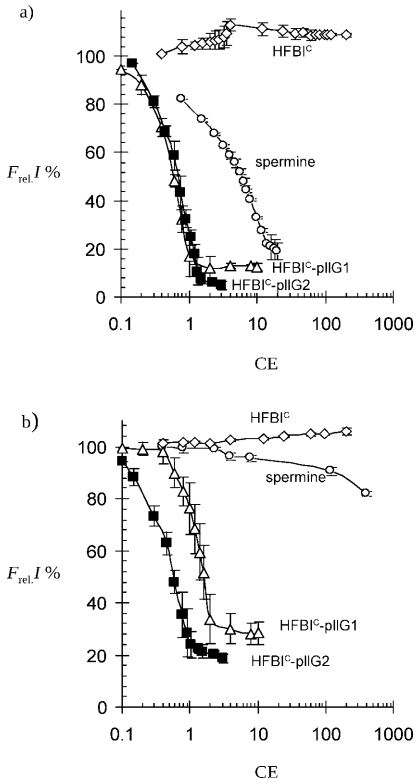

Figure 3. Ethidium bromide fluorescence quenching results for spermine, HFBI^C, HFBI^C–**pIIG1** and HFBI^C–**pIIG2**. Quenching of ethidium bromide fluorescence in the presence of a) 9.4 and b) 150 mM NaCl. The results are the average of three individual titrations; error bars: standard deviation.

Table 1. CE_{50} values for spermine, HFBI^C, HFBI^C–**pIIG1**, and HFBI^C–**pIIG2** as determined by an ethidium bromide displacement assay.[a]

Compound	Nominal charge	CE_{50}[b]	CE_{50}[c]
spermine	4+	6	>400
HFBI^C	(4+)[d]	>200	>200
HFBI^C–**pIIG1**	9+	0.6	1.6
HFBI^C–**pIIG2**	27+	0.6	0.6

[a] Conditions: buffered water pH 7.2 (2 mM 4-(2-hydroxyethyl)-1-piperazineethanesulfonic acid (HEPES), 0.05 mM EDTA), DNA (1 μM), and EthBr (1.26 μM). Total added polyamine solution did not exceed 5% of the total volume, thus corrections were not made for sample dilution. Results are an average of three titrations. [b] In the presence of 9.4 mM NaCl. [c] In the presence of 150 mM NaCl. [d] According to the protein amino acid sequence and the number of protonatable side chains, four positive charges were assumed for comparison.

CE_{50} values for HFBI^C–**pIIG1** and HFBI^C–**pIIG2** in the presence of 150 mM NaCl are 1.6 and 0.6, respectively. HFBI^C–**pIIG1** clearly loses some of its binding affinity at physiological NaCl concentrations. Increasing the salt concentration results in decreased Debye screening lengths, and consequently only multivalent compounds with high local concentration of binding ligands are able to efficiently interact with DNA. As expected, HFBI^C–**pIIG2** is able to maintain its high binding affinity towards DNA even in the presence of 150 mM NaCl. The binding affinity for the second-generation conjugate is better than that of the first generation, a trend that we have observed with similar previously reported spermine dendrons.[30–35] These binding observations agree well with our previously reported protein–dendron conjugates.

Due to the complex nature of multivalent interactions, experimental insight into the binding is challenging to obtain. Thus, we decided to apply a molecular dynamics (MD) modeling approach to obtain the thermodynamic parameters of HFBI^C–**pIIG1** and HFBI^C–**pIIG2** binding to DNA. All simulations were carried out under periodic conditions and in the presence of 9.4 or 150 mM NaCl (see the Supporting Information for computational details). All energetic analyses for each molecular system were calculated for 200 snapshots taken from the equilibrated phase of a single 10 ns MD trajectory. The free energy of binding (ΔG_{bind}) was calculated with the Molecular Mechanics/Poisson–Boltzmann surface area method,[36] as given in Equation (1). The average values of the enthalpic contribution (ΔH_{bind}) to ΔG_{bind} were calculated by summing the gas phase in vacuo nonbond energies composed of an electrostatic and a van der Waals term ($\Delta E_{gas}=\Delta E_{ele}+\Delta E_{vdw}$) and the solvation free energies ($\Delta G_{solv}=\Delta G_{PB}+\Delta G_{NP}$)[37] as described by Equation (2).

$$\Delta G_{bind} = \Delta H_{bind} - T\Delta S_{bind} \quad (1)$$

$$\Delta H_{bind} = \Delta E_{gas} + \Delta G_{sol} \quad (2)$$

The polar component (ΔG_{PB}) was evaluated by using the Poisson–Boltzmann approach,[38] whereas the non-polar contribution (ΔG_{NP}) to the solvation energy was calculated as $\Delta G_{NP}=\gamma(SASA)+\beta$, in which $\gamma=0.00542$ kcal Å^{-2}, $\beta=0.92$ kcal mol^{-1}, and SASA is the solvent-accessible surface area that was calculated with the MSMS program.[39] Finally, the normal-mode analysis approach was applied to 100 MD frames to estimate the entropic contributions ($-T\Delta S$).[40]

Thermodynamic parameters for the binding of HFBI^C–**pIIG1** and HFBI^C–**pIIG2** are presented in Table 2. The values are normalized by the nominal charge on the dendron to allow a direct comparison between the binding values of different dendron generations. From the data, it is evident that the high binding affinity for each system is almost completely driven by a strong favorable binding enthalpy (negative), which is opposed by unfavorable binding entropy (negative). The $\Delta G_{bind}/N$ values are in good agree-

Table 2. Thermodynamic parameters determined by molecular dynamics methods for the binding of DNA.[a]

Compound	[NaCl] [mM]	$\Delta H_{bind}/N$	$-T\Delta S_{bind}/N$	$\Delta G_{bind}/N$
HFBI^C–**pIIG1**	9.4	−11.4±2.0	3.8±1.0	−7.7
HFBI^C–**pIIG2**	9.4	−12.5±1.0	4.7±0.8	−7.8
HFBI^C–**pIIG1**	150	−11.2±1.0	6.9±1.6	−4.3
HFBI^C–**pIIG2**	150	−11.3±0.4	3.6±0.7	−7.7

[a] $\Delta H_{bind}/N$, $-T\Delta S_{bind}/N$ and $\Delta G_{bind}/N$ are the total enthalpic, entropic, and free energies of binding (ΔH_{bind}, $-T\Delta S_{bind}$, and ΔG_{bind}) normalized per charged amine (see Table 1 for the nominal charge) to allow comparison of the energetics between different generations. All energies are expressed in kcal mol^{-1}.

ment with the CE_{50} values presented in Table 1. HFBI^C–**pllG1** loses some of its binding affinity when the salt concentration is increased, but interestingly this is due to the entropic cost ($-T\Delta S$), which increased by 2.2 kcal mol^{-1}. Increasing the salt concentration does not affect $\Delta G_{bind}/N$ of HFBI^C–**pllG2**. The enthalpic terms for each system are similar at ≈ -11.3 kcal mol^{-1}. An exception to this is HFBI^C–**pllG2**, which has a higher $\Delta H_{bind}/N$ value of -12.5 kcal mol^{-1} in the presence of 9.4 mM NaCl. However, the more favorable binding enthalpy is compensated by a higher entropic cost. Binding of HFBI^C–**pllG1** and HFBI^C–**pllG2** to DNA is illustrated in Figure 4 by snapshots of the MD simulations.

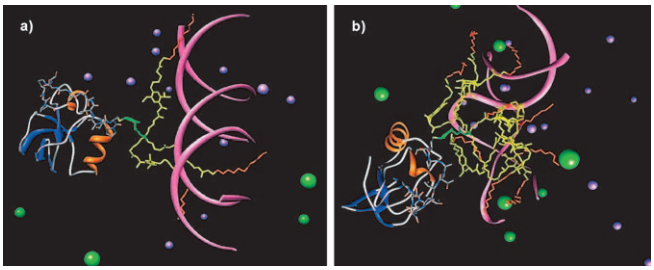

Figure 4. Snapshots of MD simulation of a) HFBI^C–**pllG1** and b) HFBI^C–**pllG2** binding to DNA in the presence of NaCl (150 mM). Core, frame, and spermine ligands of the dendron are represented in green, yellow, and red, respectively. HFBI^C and DNA (pink) are represented as solid ribbons. Only those ions in close proximity to the binding site are present in the pictures. Cl^- ions are green, and Na^+ ions are purple; water molecules and hydrogen atoms have been removed for clarity.

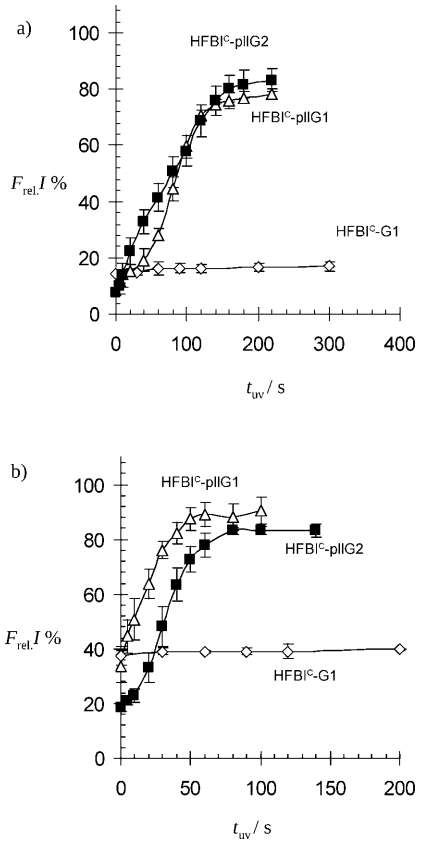

Figure 5. Ethidium bromide fluorescence enhancement: release of DNA from the complexes as a function of the UV irradiation time in the presence of a) 9.4 and b) 150 mM NaCl. The results are the average of three individual titrations; error bars: standard deviation.

Importantly, all of the MD simulations are able to reproduce the experimentally observed binding behavior and are in line with our previous modeling results,[41] which indicates that the models are reliable.

The disassembly of the complex and release of DNA was then directly monitored by using EthBr assay as a function of UV exposure time (Figure 5). Disassembly of the protein–DNA complexes is based on the photochemical degradation of the dendron and the release of the DNA can, therefore, take place due to two factors. First, the cationic polyamine groups are attached to the dendritic scaffold through an *o*-nitrobenzyl linker that undergoes photocleavage when irradiated with long-wavelength UV light. Optically triggered release of the cationic surface groups destroys the multivalent supramolecular interactions between DNA and the dendron, which leaves only individual surface groups with a weak affinity towards DNA. Second, the cleavage reaction leaves an anionic polycarboxylic acid on the dendron surface, which will further repel the negatively charged DNA (Figure 1b,e).

Here, DNA release can be observed as an increase in the EthBr fluorescence when re-intercalation into DNA becomes possible. DNA release can, therefore, be directly monitored over time. DNA was first fully complexed with HFBI^C–**pllG1**, HFBI^C–**pllG2**, and HFBI^C–**G1** (a previously reported conjugate of HFBI and a first-generation Newkome-type dendron with three spermine groups and no photolabile linkers[32]) to CE = 3. The complexes were then exposed to UV light and the increase in EthBr fluorescence was monitored after different time periods in the presence of 9.4 and 150 mM NaCl. At both NaCl concentrations, a clear increase in the EthBr fluorescence was observed. In the presence of 9.4 mM NaCl, HFBI^C–**pllG1** and HFBI^C–**pllG2** release DNA in a similar manner after exposure to UV for approximately 180 s (Figure 5a). A similar DNA release is observed when the DNA is complexed with scFv^C–**pllG1** (see the Supporting Information). As expected, the release in the presence of 150 mM NaCl is slightly faster and consequently HFBI^C–**pllG1** and HFBI^C–**pllG2** are able to release DNA after 60 and 80 s, respectively (Figure 5b). Importantly, no DNA release was observed with the nondegradable HFBI^C–**G1** control in any experiment, indicating that the DNA release is indeed due to the cleavage of the *o*-nitrobenzyl linker and consequent degradation of the multivalent binding surface.

DNA binding and release was also demonstrated by using a gel electrophoresis retardation assay (Figure 6). In this experiment HFBI^C–**pllG1**, HFBI^C–**pllG2**, and HFBI^C–**G1** can also complex DNA, which is observed as decrease in the electrophoretic mobility (Figure 6a, lanes 2–4). However, in the samples that had been treated with UV light, only pho-

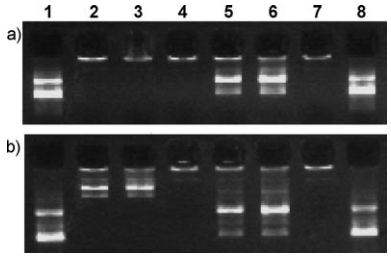

Figure 6. Gel electrophoresis of plasmid DNA (150 ng per lane). a) Lanes 1 and 8: pDNA; lane 2: pDNA + HFBI^{C}–**pllG1** (CE = 3); lane 3: pDNA + HFBI^{C}–**pllG2** (CE = 3); lane 4: pDNA + HFBI^{C}–**G1** (CE = 3); lane 5: pDNA + HFBI^{C}–**pllG1** (CE = 3) + UV (1 min); lane 6: pDNA + HFBI^{C}–**pllG2** (CE = 3) + UV (1 min); lane 7: pDNA + HFBI^{C}–**G1** (CE = 3) + UV (1 min). b) Gel a) after UV exposure and electrophoresis for an additional 20 min.

tolabile dendrons HFBI^{C}–**pllG1** and HFBI^{C}–**pllG2** were able to release DNA (Figure 6a, lanes 5,6) whereas HFBI^{C}–**G1** could not. Figure 6b shows the gel presented in Figure 6a after being exposed to UV light and subjected to an additional 20 min of electrophoresis. Lanes 2 and 3 (Figure 6b) clearly show that the DNA can be released from the complex in situ, even inside the gel.

Conclusion

We present a method for temporary adhesion of proteins to DNA, in which multivalent dendrons bind the two species together through multiple electrostatic interactions. Experimental work combined with molecular dynamics modeling demonstrated that the binding strength is dependent on the generation of the dendron, with more highly branched dendrons exhibiting higher activity. Importantly, the high-affinity binding interactions can be degraded by short exposure to UV ($\lambda \approx 350$ nm), which induces the controlled cleavage of *o*-nitrobenzyl-linked surface groups from the dendron scaffold and allows the DNA and the protein particles to be released. This approach can open new strategies to control the interactions between biomolecules and lead to the development of stimuli-responsive carriers for biomedical applications.

Experimental Section

Please see the Supporting Information for the synthesis and characterization of **pllG1** and **pllG2** and the computational details.

Preparation of HFBI with a free cysteine residue (HFBI^{C}): HFBI was received from VTT Tschnical Research Centre of Finland (Espoo, Finland). Site-directed mutagenesis, production strain, production, purification, and reduction of HFBI were performed as described previously.[23,32,42,43] The resulting modified HFBI^{C} had the following sequence; SCPATTTGSSPGPSNGNGNVCPPGLFSNPQCCATQVLGLIGLDCKVPSQNVYDGTDFRNVCAKTGAQPLCCVAPVAGQALLCQTAVGA, in which the added N terminus is underlined.

HFBI^{C}–pllG1 and HFBI^{C}–pllG2: A typical procedure for conjugation of HFBI^{C} and **pllG1** is described below. Conjugation of **pllG1** with HFBI^{C} was carried out in buffered H_2O; **pllG1** (5 mg, 2.26 μmol) was dissolved in 100 μL H_2O and mixed with buffered H_2O (400 μL, 0.2 M NaP pH 7; 111 μL, 0.5 M EDTA, pH 7.52). The mixture was then combined with a solution of HFBI^{C} (4 mg, 0.46 μmol) in H_2O (400 μL), sonicated briefly in an ultrasonicator bath, and left standing at RT for 16 h.

The HFBI^{C} and HFBI^{C}–dendron conjugates were purified by using a preparative RP-HPLC system coupled to a UV/Vis detector probing at $\lambda = 215$, 230, and 280 nm (Äkta explorer) by using a Vydac C4 (1 × 20 cm) column and a gradient elution from 0→100 % of eluent B in A (eluent A: 0.1 % trifluoroacetic acid in H_2O; eluent B: 0.1 % trifluoroacetic acid in MeCN). Peak fractions were pooled and lyophilized. The identity of the protein was confirmed by using MALDI-TOF mass spectrometry (see the Supporting Information for details). Analytical HPLC samples were analyzed by using the same Äkta system equipped with a 4.6 mm × 5 cm Vydac C4 column. Blank H_2O was subtracted from each sample.

Preparation of scFv with a free cysteine residue (scFv^{C}): Batch-scale expression of anti-HER2 scFv^{C} (for the sequence, see: HumAb4D5–8 clone[44]) was done with the *E. coli* RV308 strain under optimized growth conditions. First, the scFv^{C} clone was grown in Luria Bertani medium (20 mL) supplemented with ampicillin (100 μg mL^{-1}) and glucose (1 % v/v) for 16 h at 37 °C and 220 rpm, then diluted (1:50) in 3 L Erlenmeyer flasks with a fresh terrific broth medium that contained ampicillin (100 μg mL^{-1}) and grown at 37 °C and 220 rpm until the OD600 reached 4.0–5.0. The induction of scFv^{C} expression was done with 1 mM IPTG (isopropyl β-D-1-thiogalactopyranoside), which was added to the medium together with ampicillin (100 μg mL^{-1} final concentration). The flasks were incubated for 16 h at 30 °C and 220 rpm. The cells were harvested by centrifugation (Sorvall RC6) with a GS-3 rotor at 4 °C and 13700*g* for 15 min. The anti-Her2 scFv^{C} was purified directly from the culture medium by using IMAC, as follows: first, the culture medium was diluted 1:1 with 2× IMAC buffer (glycerol (20 % v/v), NaCl (2 M), HEPES (20 mM), imidazole (2 mM); pH 7.4). Ni^{2+}-loaded Sepharose slurry (GE Healthcare; 15 mL L^{-1} of culture medium) was added to the diluted medium, and the bottles were placed on an end-over-end shaker for 16 h at 4 °C. The Ni^{2+}-loaded Sepharose slurry was removed on a standard gel chromatography column and the bound protein was washed out with an increasing imidazole gradient (1→500 mM).

scFv^{C}–pllG1: Before conjugation with **pllG1**, the C-terminal cysteine of scFv^{C} was reduced by adding dithiothreitol (DTT; 2 mM final concentration) and incubating the protein at 37 °C for 30 min. The sample was then loaded onto a desalting column (BioRad) and eluted with one portion of PBS (phosphate buffer saline; 4 mL, pH 6.0) that contained EDTA (1 mM). Fractions of 200–500 μL were collected, the protein content was measured photometrically (A280), and the peak fractions were pooled and conjugated in 2:1 molar ratio of **pllG1** and scFv^{C} respectively. The reaction mixture was first incubated for 1–2 h at RT and then for 16 h at 4 °C.

The purification of conjugates from unconjugated scFv^{C} and free **pllG1** was carried out by fast protein liquid chromatography (FPLC). The conjugate solution was loaded with a pump onto a chromatography column (BioRad) that contained High-S support ion exchange matrix (BioRad). The elution was done with a buffer gradient that was preceded by washing the column until a baseline emerged from the graph blotter with A280 detection. The scFv^{C}-**pllG1** conjugate was eluted with a concentration gradient of 0.1–2 M NaCl in HEPES (20 mM) and EDTA (20 mM) at pH 7.0. According to the elution curve, relevant fractions were first checked with SDS-PAGE to validate the conjugate, then the peak fractions were pooled and dialyzed (molecular weight cut-off 12–14 kDa; Medicel) against HEPES (10 mM, pH 7.0). The final solution was concentrated in dialysis tubing placed on solid PEG6000 until A280 ≈ 0.3. The identity of the conjugate was confirmed with MALDI-TOF mass spectrometry (see the Supporting Information).

Ethidium bromide displacement assay: A Varian Cary Eclipse spectrofluorometer was used to collect the data. Excitation of the sample was carried out in a 3 mL quartz cuvette with excitation at $\lambda = 546$ nm, and the emission was measured at $\lambda = 595$ nm. The buffer designated 0.01 SHE had an ionic strength of 0.01 and contained HEPES (2 mM), EDTA (10 μM), and NaCl (9.4 mM), and the pH was adjusted to 7.2 with

NaOH. The biological SHE contained HEPES (2 mM), EDTA (10 μM), and NaCl (150 mM), and the pH was adjusted to 7.2 with NaOH. Ethidium bromide (1.26 μM) was then dissolved in the buffer. After mixing, the fluorescence was measured. Type III DNA from salmon testes (1 mM in 0.01 SHE) was added to give a nucleotide concentration of 1 μM and increase the fluorescence to measurement maxima. A molecular weight of 330 g mol^{-1} and one negative charge per nucleotide were assumed. Each fluorescence measurement was repeated twice, each titration series was repeated three times, and the results were averaged. The added test compound solution volumes did not exceed 5% of the total volume and thus corrections were not made for sample dilution. Here, charge excess (CE) is defined as the nominal "number of positive charges" of the polyamine divided by the "number of negative charges" present on the DNA. A molecular weight of 330 g mol^{-1} and one negative charge per nucleotide were assumed. CE_{50} values indicate the nominal dendron charge excess causing a 50% decrease in fluorescence intensity.

Ethidium bromide displacement (Figure 3): The aqueous test agent (spermine, $HFBI^{C}$, $HFBI^{C}$–**pllG1** $HFBI^{C}$–**pllG2**, and $scFv^{C}$–**pllG1**) was added in small portions to reduce the fluorescence of DNA–ethidium complex to 50% (or plateau).

Complex degradation with UV irradiation (Figure 5): DNA was first completely complexed with the test agent to CE = 3, resulting in EthBr displacement and a decrease in fluorescence. Complexes were then irradiated with UV light to degrade the photolabile dendrons, resulting in EthBr reintercalation and increase in fluorescence. EthBr fluorescence was recorded after different time periods.

UV light irradiation: Samples were irradiated in quartz cuvettes for different time periods by using a Rayonet photochemical reactor (Southern New England Ultraviolet, Middletown, CT, USA) equipped with 16 RPR-3500 Å lamps (intensity approximately 9.2 mW cm^{-2}, $\lambda = 350$ nm).

Gel retardation assay: Appropriate amounts of protein–dendron conjugate and DNA plasmid (250 ng, 6.7 kbp expression vector, gWiz-Luc (Aldevron, Fargo, ND, USA)) in SHE (150 mM) were added to another portion of SHE (10 μL, 150 mM) to achieve the desired polyamine/DNA ratio. The resultant complexes were incubated at RT for 5 min. Loading dye (2 μL) was added and the mixtures were incubated at RT for a further 5 min, after which an aliquot (15 μL) was run on a 0.8% agarose gel (70 V, 20 min). DNA was visualized by using ethidium bromide staining (Bio-Rad, Hercules, CA).

Acknowledgements

This work was supported by the Academy of Finland, Instrumentarium Science Foundation, and the Alfred Kordelin Foundation. We acknowledge Prof. M. B. Linder, Prof. O. Ikkala, Prof. O. Kallioniemi, and Prof. A. Danani for discussions and support.

[1] S. C. Glotzer, M. J. Solomon, *Nat. Mater.* **2007**, *6*, 557–562.
[2] A. Walther, A. H. E. Muller, *Soft Matter* **2008**, *4*, 663–668.
[3] Z. Zhang, W. Dayang, M. Helmuth, *Angew. Chem.* **2005**, *117*, 7945–7948; *Angew. Chem. Int. Ed.* **2005**, *44*, 7767–7770.
[4] A. M. Jackson, Y. Hu, P. J. Silva, F. Stellacci, *J. Am. Chem. Soc.* **2006**, *128*, 11135–11149.
[5] C. J. Loweth, W. B. Caldwell, X. Peng, A. P. Alivisatos, P. G. Schultz, *Angew. Chem.* **1999**, *111*, 1925–1929; *Angew. Chem. Int. Ed.* **1999**, *38*, 1808–1812.
[6] V. N. Manoharan, M. T. Elsesser, D. J. Pine, *Science* **2003**, *301*, 483–487.
[7] Z. L. Ding, R. B. Fong, C. J. Long, P. S. Stayton, A. S. Hoffman, *Nature* **2001**, *411*, 59–62.
[8] K. L. Heredia, H. D. Maynard, *Org. Biomol. Chem.* **2007**, *5*, 45–53.
[9] G. G. Kochendoerfer, *Curr. Opin. Chem. Biol.* **2005**, *9*, 555–560.
[10] T. Shimoboji, E. Larenas, T. Fowler, A. S. Hoffman, P. S. Stayton, *Bioconjugate Chem.* **2003**, *14*, 517–525.
[11] C. Niemeyer, M. M. Adler, *Angew. Chem.* **2002**, *114*, 3933–3937; *Angew. Chem. Int. Ed.* **2002**, *41*, 3779–3783.
[12] C. M. Niemeyer, *Chem. Eur. J.* **2001**, *7*, 3188–3195.
[13] C. M. Niemeyer, *Angew. Chem.* **2010**, *122*, 1220–1238; *Angew. Chem. Int. Ed.* **2010**, *49*, 1200–1216.
[14] C. C. Lee, J. A. MacKay, J. M. J. Frechet, F. C. Szoka, *Nat. Biotechnol.* **2005**, *23*, 1517–1526.
[15] L. L. Kiessling, J. E. Gestwicki, L. E. Strong, *Curr. Opin. Chem. Biol.* **2000**, *4*, 696–703.
[16] P. I. Kitov, D. R. Bundle, *J. Am. Chem. Soc.* **2003**, *125*, 16271–16284.
[17] P. I. Kitov, J. M. Sadowska, G. Mulvey, G. D. Armstrong, H. Ling, N. S. Pannu, R. J. Read, D. R. Bundle, *Nature* **2000**, *403*, 669–672.
[18] M. Mammen, S.-K. Choi, G. M. Whitesides, *Angew. Chem.* **1998**, *110*, 2908–2953; *Angew. Chem. Int. Ed.* **1998**, *37*, 2754–2794.
[19] A. Levskaya, O. D. Weiner, W. A. Lim, C. A. Voigt, *Nature* **2009**, *461*, 997–1001.
[20] R. J. Amir, N. Pessah, M. Shamis, D. Shabat, *Angew. Chem.* **2003**, *115*, 4632–4637; *Angew. Chem. Int. Ed.* **2003**, *42*, 4494–4499.
[21] F. M. H. de Groot, C. Albrecht, R. Koekkoek, P. H. Beusker, H. W. Scheeren, *Angew. Chem.* **2003**, *115*, 4628–4632; *Angew. Chem. Int. Ed.* **2003**, *42*, 4490–4494.
[22] M. L. Szalai, D. V. McGrath, *Tetrahedron* **2004**, *60*, 7261–7266.
[23] J. Hakanpää, G. R. Szilvay, H. Kaljunen, M. Maksimainen, M. Linder, J. Rouvinen, *Protein Sci.* **2006**, *15*, 2129–2140.
[24] M. B. Linder, *Curr. Opin. Colloid Interface Sci.* **2009**, *14*, 356–363.
[25] M. B. Linder, G. R. Szilvay, T. Nakari-Setälä, M. E. Penttilä, *FEMS Microbiol. Rev.* **2005**, *29*, 877–896.
[26] H. A. B. Wosten, *Annu. Rev. Microbiol.* **2001**, *55*, 625–646.
[27] A. Paananen, E. Vuorimaa, M. Torkkeli, M. Penttilä, M. Kauranen, O. Ikkala, H. Lemmetyinen, R. Serimaa, M. B. Linder, *Biochemistry* **2003**, *42*, 5253–5258.
[28] D. Chandler, *Nature* **2005**, *437*, 640–647.
[29] J. G. Hardy, M. A. Kostiainen, D. K. Smith, N. P. Gabrielson, D. W. Pack, *Bioconjugate Chem.* **2006**, *17*, 172–178.
[30] M. A. Kostiainen, J. G. Hardy, D. K. Smith, *Angew. Chem.* **2005**, *117*, 2612–2615; *Angew. Chem. Int. Ed.* **2005**, *44*, 2556–2559.
[31] M. A. Kostiainen, G. R. Szilvay, J. Lehtinen, D. K. Smith, M. B. Linder, A. Urtti, O. Ikkala, *ACS Nano* **2007**, *1*, 103–113.
[32] M. A. Kostiainen, G. R. Szilvay, D. K. Smith, M. B. Linder, O. Ikkala, *Angew. Chem.* **2006**, *118*, 3618–3622; *Angew. Chem. Int. Ed.* **2006**, *45*, 3538–3542.
[33] M. A. Kostiainen, D. K. Smith, O. Ikkala, *Angew. Chem.* **2007**, *119*, 7744–7748; *Angew. Chem. Int. Ed.* **2007**, *46*, 7600–7604.
[34] D. J. Welsh, S. P. Jones, D. K. Smith, *Angew. Chem.* **2009**, *121*, 4107–4111; *Angew. Chem. Int. Ed.* **2009**, *48*, 4047–4051.
[35] M. A. Kostiainen, H. Rosilo, *Chem. Eur. J.* **2009**, *15*, 5656–5660.
[36] J. Srinivasan, T. E. Cheatham, P. Cieplak, P. A. Kollman, D. A. Case, *J. Am. Chem. Soc.* **1998**, *120*, 9401–9409.
[37] B. Jayaram, D. Sprous, D. L. Beveridge, *J. Phys. Chem. B* **1998**, *102*, 9571–9576.
[38] D. Sitkoff, K. A. Sharp, B. Honig, *J. Phys. Chem.* **1994**, *98*, 1978–1988.
[39] M. F. Sanner, A. J. Olson, J.-C. Spehner, *Biopolymers* **1996**, *38*, 305–320.
[40] I. Andricioaei, M. Karplus, *J. Chem. Phys.* **2001**, *115*, 6289–6292.
[41] G. M. Pavan, A. Danani, S. Pricl, D. K. Smith, *J. Am. Chem. Soc.* **2009**, *131*, 9686–9694.
[42] M. Linder, K. Selber, T. Nakari-Setälä, Q. Mingqiang, M.-R. Kula, M. Penttilä, *Biomacromolecules* **2001**, *2*, 511–517.
[43] M. Linder, G. R. Szilvay, T. Nakari-Setälä, H. Söderlund, M. Penttilä, *Protein Sci.* **2002**, *11*, 2257–2266.
[44] P. Carter, L. Presta, C. M. Gorman, J. B. Ridgway, D. Henner, W. L. Wong, A. M. Rowland, C. Kotts, M. E. Carver, H. M. Shepard, *Proc. Natl. Acad. Sci. USA* **1992**, *89*, 4285–4289.

Received: January 14, 2010
Published online: April 30, 2010

